

Systematic Errors in Future Weak Lensing Surveys: Requirements and Prospects for Self-Calibration

Dragan Huterer

*Kavli Institute for Cosmological Physics and Astronomy and
Astrophysics Department, University of Chicago, Chicago, IL 60637*

Masahiro Takada

Astronomical Institute, Tohoku University, Sendai 980-8578, Japan

Gary Bernstein and Bhuvnesh Jain

Department of Physics and Astronomy, University of Pennsylvania, Philadelphia, PA 19104

We study the impact of systematic errors on planned weak lensing surveys and compute the requirements on their contributions so that they are not a dominant source of the cosmological parameter error budget. The generic types of error we consider are multiplicative and additive errors in measurements of shear, as well as photometric redshift errors. In general, more powerful surveys have stronger systematic requirements. For example, for a SNAP-type survey the multiplicative error in shear needs to be smaller than 1% $(f_{\text{sky}}/0.025)^{-1/2}$ of the mean shear in any given redshift bin, while the centroids of photometric redshift bins need to be known to better than 0.003 $(f_{\text{sky}}/0.025)^{-1/2}$. With about a factor of two degradation in cosmological parameter errors, future surveys can enter a self-calibration regime, where the mean systematic biases are self-consistently determined from the survey and only higher-order moments of the systematics contribute. Interestingly, once the power spectrum measurements are combined with the bispectrum, the self-calibration regime in the variation of the equation of state of dark energy w_a is attained with only a 20-30% error degradation.

I. INTRODUCTION

There has been significant recent progress in the measurements of weak gravitational lensing by large scale structure. Only five years after the first detections made by several groups (Wittman et al. 2000, Bacon et al. 2000, van Waerbeke et al. 2000, Kaiser et al. 2000), weak lensing already imposes strong constraints on the matter density relative to critical Ω_M and the amplitude of mass fluctuations σ_8 (Hoekstra, Yee & Gladders 2002, Jarvis et al. 2003, Rhodes et al. 2004, Heymans et al. 2004; for a review see Refregier 2003), as well as the first interesting constraints on the equation of state of dark energy (Jarvis et al. 2005).

The main advantage of weak lensing is that it directly probes the distribution of matter in the universe. This makes weak lensing a powerful probe of cosmological parameters, including those describing dark energy (Hu & Tegmark 1999, Huterer 2002, Hu 2003a, Heavens 2003, Refregier et al. 2003, Benabed & Van Waerbeke 2004, Takada & Jain 2004, Takada & White 2004, Song & Knox 2004, Ishak et al. 2004, Ishak 2005). The weak lensing constraints are especially effective when some redshift information is available for the source galaxies; use of redshift tomography can improve the cosmological constraints by factors of a few (Hu 1999). Furthermore, measurements of the weak lensing bispectrum (Takada & Jain 2004) and purely geometrical tests (Jain & Taylor 2003, Bernstein & Jain 2004, Zhang et al. 2003, Song & Knox 2004, Hu & Jain 2004, Bernstein 2005) lead to significant improvements of accuracy in measuring the cosmological parameters. When these methods are combined, weak lensing by itself is expected to constrain the equation of state of dark energy w to a few percent, and impose interesting constraints on the time variation of w . Ongoing or planned surveys, such as the Canada-France-Hawaii Telescope Legacy Survey¹, the Dark Energy Survey² (DES), PanSTARRS³ and VISTA⁴ are expected to significantly extend lensing measurements, while the ultimate precision will be achieved with the SuperNova/Acceleration Probe⁵ (SNAP; Aldering et al. 2004) and the Large Synoptic Survey Telescope⁶ (LSST).

However, so far the rosy weak lensing parameter accuracy predictions that have appeared in literature have not

¹ <http://www.cfht.hawaii.edu/Science/CFHLS>

² <http://cosmology.astro.uiuc.edu/DES>

³ <http://pan-starrs.ifa.hawaii.edu>

⁴ <http://www.vista.ac.uk>

⁵ <http://snap.lbl.gov>

⁶ <http://www.lsst.org>

allowed for the presence of systematics (exceptions are Ishak et al. (2004) and Knox et al. (2005) who consider a shear calibration error, and Bernstein (2005) who does the same for the cross-correlation cosmography of weak lensing). This is not surprising, as we are just starting to understand and study the full budget of systematic errors present in weak lensing measurements. Nevertheless, some recent work has addressed various aspects of the systematics, both experimental and theoretical, and ways to correct for them. For example, Vale et al. (2004) estimated the effects of extinction on the extracted shear power spectrum, while Hirata & Seljak (2003), Hoekstra (2004) and Jarvis & Jain (2004) considered the errors in measurements of shear. Several studies explored the effect of theoretical uncertainties (White 2004, Zhan & Knox 2004, Huterer & Takada 2004) and ways to protect against their effects (Huterer & White 2005). It has been pointed out that second-order corrections in the shear predictions can be important (Schneider et al. 2002, Hamana et al. 2002, Cooray & Hu 2002, White 2005, Dodelson & Zhang 2005, Dodelson et al. 2005).

Despite these efforts, we are at an early stage in our understanding of weak lensing systematics. Realistic assessments of systematic errors is likely to impact strategies for measuring the weak lensing shear (Bernstein 2002, Bernstein & Jarvis 2002, Rhodes et al. 2004, Mandelbaum et al. 2005). Eventually we would like to bring weak lensing to the same level as cosmic microwave background anisotropies (CMB) and type Ia supernovae, where the systematic error budget is better understood and requirements for the control of systematic precisely outlined (e.g. Tegmark et al. 2000, Hu, Hedman & Zaldarriaga 2003, Kim et al. 2003, Linder & Miquel 2004).

The purpose of this paper is to introduce the framework for the discussion of systematic errors in weak lensing measurements and outline requirements for several generic types of systematic error. The reason that we do *not* consider specific sources of error (e.g. temporal variations in the telescope optics or fluctuations in atmospheric seeing) is that there are many of them, they strongly depend on a particular survey considered, and they are often poorly known before the survey has started collecting data. Instead we argue that, at this early stage of our understanding of weak lensing systematics, it is more practical and useful to consider three generic types of error – multiplicative and additive error in measurements of shear, as well as redshift error. These generic errors are useful intermediate quantities that link actual experimental sources of error to their impact on cosmological parameter accuracy. In fact, realistic systematic errors for any particular experiment can in general be converted to these three generic systematics. Given the specifications of a particular survey, one can then estimate how much a given systematic degrades cosmological parameters. This can be used to optimize the design of the experiment to minimize the effects of systematic errors on the accuracy of desired parameter. For example, accurate photometric redshift requirements will lead to requirements on the number of filters and their wavelength coverage. Similarly, the requirements on multiplicative and additive errors in shear will determine how accurate the sampling of the point spread function needs to be.

The plan of the paper is as follows. In § II we discuss the survey specifications and cosmological parameters in this study. In § III we describe the parameterization of systematic errors. In § IV-VI we present the requirements on the systematic errors for the power spectrum, while in § VII we study the requirements when both the power spectrum and the bispectrum are used. We combine the redshift and multiplicative errors and discuss trends in § VIII and conclude in § IX.

II. METHODOLOGY, COSMOLOGICAL PARAMETERS AND FIDUCIAL SURVEYS

We express the measured convergence power spectrum as

$$\hat{C}_{ij}^{\kappa}(\ell) = \hat{P}_{ij}^{\kappa}(\ell) + \delta_{ij} \frac{\sigma_{\gamma}^2}{\bar{n}_i}, \quad (1)$$

where $\hat{P}_{ij}^{\kappa}(\ell)$ is the measured power spectrum with systematics (see the next Section on how it is related to the no-systematic power spectrum $P_{ij}^{\kappa}(\ell)$), σ_{γ}^2 is the variance of each component of the galaxy shear and \bar{n}_i is the average number of resolved galaxies in the i th redshift bin per steradian. The convergence power spectrum at a fixed multipole ℓ and for the i th and j th redshift bin is given by

$$P_{ij}^{\kappa}(\ell) = \int_0^{\infty} dz \frac{W_i(z) W_j(z)}{r(z)^2 H(z)} P\left(\frac{\ell}{r(z)}, z\right), \quad (2)$$

where $r(z)$ is the comoving angular diameter distance and $H(z)$ is the Hubble parameter. The weights W_i are given by

$$W_i(\chi) = \frac{3}{2} \Omega_M H_0^2 g_i(\chi) (1+z) \quad (3)$$

	DES	SNAP	LSST
Area (sq. deg.)	5000	1000	15000
n (gal/arcmin ²)	10	100	30
σ_γ	0.16	0.22	0.22
z_{peak}	0.5	1.0	0.7

TABLE I: Fiducial sky coverage, density of source galaxies, variance of (each component of) shear of one galaxy, and peak of the source galaxy redshift distribution for the three surveys considered.

where $g_i(\chi) = r(\chi) \int_\chi^\infty d\chi_s n_i(\chi_s) r(\chi_s - \chi) / r(\chi_s)$, χ is the comoving radial distance and n_i is the fraction of galaxies assigned to i th redshift bin. We employ the redshift distribution of galaxies of the form

$$n(z) \propto z^2 \exp(-z/z_0) \quad (4)$$

where z_0 is survey dependent and specified below. The cosmological constraints can then be computed from the Fisher matrix

$$F_{ij} = \sum_\ell \left(\frac{\partial \mathbf{C}}{\partial p_i} \right)^T \mathbf{Cov}^{-1} \frac{\partial \mathbf{C}}{\partial p_j}, \quad (5)$$

where \mathbf{C} is the column matrix of the observed power spectra and \mathbf{Cov}^{-1} is the inverse of the covariance matrix between the power spectra whose elements are given by

$$\text{Cov} \left[\hat{C}_{ij}^\kappa(\ell'), \hat{C}_{kl}^\kappa(\ell) \right] = \frac{\delta_{\ell\ell'}}{(2\ell+1) f_{\text{sky}} \Delta\ell} \left[\hat{C}_{ik}^\kappa(\ell) \hat{C}_{jl}^\kappa(\ell) + \hat{C}_{il}^\kappa(\ell) \hat{C}_{jk}^\kappa(\ell) \right]. \quad (6)$$

Here $\Delta\ell$ is the band width in multipole we use, and f_{sky} is the fractional sky coverage of the survey.

In addition to any nuisance parameters describing the systematics, we consider six or seven cosmological parameters and assume a flat universe throughout. The six standard parameters are energy density and equation of state of dark energy Ω_{DE} and w , spectral index n , matter and baryon physical densities $\Omega_M h^2$ and $\Omega_B h^2$, and the amplitude of mass fluctuations σ_8 . Note that $w = \text{const}$ provides useful information about the sensitivity of an arbitrary $w(z)$, since the best-measured mode of any $w(z)$ is about as well measured as $w = \text{const}$ and therefore is subject to similar degradations in the presence of the systematics. It is this particular mode, being the most sensitive to generic systematics, that will drive the accuracy requirements – we explicitly illustrate this in Fig. 2. In addition to the constant w case, we also consider a commonly used two-parameter description of dark energy $w(z) = w_0 + w_a z / (1+z)$ (Linder 2003) where w_a becomes the seventh cosmological parameter in the analysis. Throughout we consider lensing tomography with 7-10 equally spaced redshift bins (see below), and we use the lensing power spectra on scales $50 \leq \ell \leq 3000$. We hold the total neutrino mass fixed at 0.1 eV; the results are somewhat dependent on the fiducial mass. We compute the linear power spectrum using the fitting formulae of Eisenstein & Hu (1999). We generalize the formulae to $w \neq -1$ by appropriately modifying the growth function of density perturbations. To complete the calculation of the full nonlinear power spectrum we use the fitting formulae of Smith et al. (2003).

The fiducial surveys, with parameters listed in Table II, are: the Dark Energy Survey; SNAP; and LSST. Note that there is some ambiguity in the definition of the number density of galaxies n_g ; it is the quantity σ_γ^2/n_g that determines the shear measurement noise level, where σ_γ is the intrinsic shape noise of each galaxy. The surveys are assumed to have the source galaxy distribution of the form in Eq. (4) which peaks at $z_{\text{peak}} = 2z_0$. For the fiducial SNAP and LSST surveys we assume tomography with 10 redshift bins equally spaced out to $z = 3$, as future photometric redshift accuracy will enable relatively fine slicing in redshift. For the DES, we assume a more modest 7 redshift bins out to $z = 2.1$, reflecting the shallower reach of the DES while keeping the redshift bins equally wide ($\Delta z = 0.3$) as in the other two surveys. Finally, we do not use weak lensing information beyond $\ell = 3000$ in order to avoid the effects of baryonic cooling (White 2004, Zhan & Knox 2004, Huterer & Takada 2004) and non-Gaussianity (White & Hu 2000, Cooray & Hu 2001), both of which contribute more significantly at smaller scales. While there may be ways to extend the useful ℓ -range to smaller scales without risking bias in cosmological constraints (Huterer & White 2005), extending the measurements to $\ell_{\text{max}} = 10000$ would improve the marginalized errors on cosmological parameters by only about

30%⁷. The parameter fiducial values and accuracies are summarized in Table II near the end of the article. The fiducial values for the parameters not listed in Table II are $\Omega_M h^2 = 0.147$, $\Omega_B h^2 = 0.021$, $n = 1.0$, and $m_\nu = 0.1\text{eV}$.

It is well known that measurements of the angular power spectrum of the CMB, such as those expected by the Planck experiment, can help weak lensing constrain the cosmological parameters. In particular, the morphology of the peaks in the CMB angular power spectrum contains useful information on the physical matter and baryon densities, while the locations of the peaks help constrain the dark energy parameters. However we checked that, when the Planck prior added, all systematics requirements become weaker (relative to those with weak lensing alone) since the Planck information is not degraded with systematic errors even if weak lensing information is. In order to be conservative, we decided not to add the Planck CMB information. Therefore, we consider the systematics requirements in weak lensing surveys alone, and note that addition of complementary information from other surveys typically weakens these requirements.

III. PARAMETERIZATION OF THE SYSTEMATICS

As mentioned above, we consider three generic sources of error. We believe that the parameterizations we propose, especially for the redshift and multiplicative shear errors, are general enough to account for the salient effects of any generic systematic. The additive shear error is more model-dependent, and while we motivate a parameterization we believe is reasonable at this time, further theoretical and experimental work needs to be done to understand additive errors.

We parameterize the redshift, multiplicative shear and additive shear errors as follows.

A. Redshift Errors

Measurements of galaxy redshifts are necessary not only for the redshift tomography – which significantly improves the accuracy in measuring dark energy parameters – but also to obtain the fiducial distribution of galaxies in redshift, $n(z)$. Therefore, understanding and correcting for the redshift uncertainties is crucial, and comparison studies between currently used photometric methods, such as that initiated by Cunha et al. (2005), are crucial.

It is important to emphasize that statistical errors in photometric redshifts do not contribute to the error budget if they are well characterized. In other words, if we know precisely the distribution of photometric redshift errors (that is, all of its moments) at *each redshift*, we can use the measured photometric distribution, $n_p(z_p)$, to recover the original spectroscopic distribution, $n(z_s)$ very precisely. In practice we will not know the redshift error distribution with arbitrary precision, rather we will typically have some prior knowledge of the mean bias and scatter at each redshift.

The quantity we consider in this paper is the uncalibrated redshift bias, that is, the residual (after correcting for the estimated bias) offset between the true mean redshift and the inferred mean photometric redshift at any given z . A more general description of the redshift error would include the scatter in the redshift error at each z . Such an analysis has recently been performed by Ma, Hu & Huterer (2005) who found that, even though the scatter is important as well, the mean bias in redshift is the dominant source of error.

Unlike Ma, Hu & Huterer (2005) who hold the overall distribution of galaxies in redshift $n(z)$ fixed and only allow variations in the tomographic bin subdivisions, we allow the redshift error to affect the overall $n(z)$ as well. At this time it is not clear how the photometric error will affect the source galaxy distribution $n(z)$ as it depends on how the source galaxy distribution will be determined. We assume that the source galaxy distribution $n(z)$ is obtained from the same photometric redshifts used to subdivide the galaxies into redshift bins. An alternative possibility is that information about the overall distribution of source galaxies is obtained from an independent source (say, another survey) while the internal photometric redshifts are only used to subdivide the overall distribution into redshift bins. The two approaches, ours and that of Ma, Hu & Huterer (2005), are therefore complementary and both should be studied. As discussed in the conclusions, it is reassuring that the two approaches give consistent results.

We consider two alternative parameterizations of the redshift error: the centroids of redshift bins, and the Chebyshev polynomial expansion of the mean bias in the $z_p - z_s$ relation. We now describe them.

Centroids of redshift bins. We first consider the centroid of each photometric redshift bin as a parameter. Any

⁷ On the other hand, especially for the DES, the Gaussian covariance assumption may be somewhat optimistic for the range $1000 < \ell < 3000$ (e.g. White & Hu 2000).

scatter in galaxy redshifts in a given tomographic bin will average out, to first order leaving the effect of an overall bias in the centroid of this bin. [Recall, the part of the bias that is uncalibrated and has not been subtracted out is what we consider here.] As discussed by Huterer et al. (2004) in the context of number-count surveys, this approach captures the salient effects of the redshift distribution uncertainty. Note, however, that the centroid shifts do not capture the “catastrophic” errors where a smaller fraction of redshifts are completely misestimated and reside in a separate island in the $z_p - z_s$ plane.

We therefore have B new parameters, where B is the number of redshift bins. To compute the Fisher derivatives for these parameters, we vary each centroid by some value dz , that is, we shift the whole bin by dz . As mentioned above, this procedure not only allows for the fact that the tomographic bin divisions are not perfectly measured, but it also deforms the overall distribution of galaxies $n(z)$.

Expansion of the redshift bias in Chebyshev polynomials. While the required accuracy of redshift bin centroids provides useful information, it is sometimes difficult to compare it with directly observable quantities. In reality, an observer typically starts with measurements of photometric redshifts which are not equal to the true, spectroscopic ones: the quantity $z_p - z_s$ may have a nonzero value — the bias — and also nonzero scatter around the biased value. Therefore, it is sometimes more useful to consider requirements on the accuracy in the $z_p - z_s$ relation.

Detailed forms of the bias and scatter are typically complicated and depend on the photometric method used and how well we are able to mimic the actual observations and correct for the biases. We write the redshift bias as a sum of N_{cheb} smooth functions — Chebyshev polynomials centered at $z_{\text{max}}/2$ and extending from $z = 0$ to $z = z_{\text{max}}$, where z_{max} (3.0 for SNAP and LSST, 2.1 for the DES) is the extent of the distribution of galaxies in redshift. [We briefly review the Chebyshev polynomials in the Appendix.] The relation between the photometric and true, spectroscopic redshifts is then

$$z_p = z_s + \sum_{i=1}^{N_{\text{cheb}}} g_i T_i(z_s^*), \quad \text{where} \quad (7)$$

$$z_s^* \equiv \frac{z_s - z_{\text{max}}/2}{z_{\text{max}}/2}, \quad (8)$$

and g_i are the coefficients that parameterize the bias. As with the centroids of redshift bins, we do not model the scatter in the $z_p - z_s$ relation as one can show that the effect of uncalibrated bias is dominant (Ma, Hu & Huterer, 2005). The effect of imperfect redshift measurements is to shift the distribution of galaxies away from the true distribution $n(z_s)$ to a biased one $n_p(z_p)$. The biased distribution of galaxies then propagates to bias the cosmological parameters. The photometric distribution can then simply be obtained from the true distribution as (e.g. Padmanabhan et al. 2005)

$$n_p(z_p) = \int_0^\infty n(z) \Delta(z_p - z, z) dz \quad (9)$$

where $\Delta(z_p - z, z)$ is the probability that the galaxy at redshift z is measured to be at redshift z_p . Since we are not modeling the scatter in the $z_p - z_s$ relation, the probability is a delta function

$$\Delta(z_p - z, z) = \delta \left(z_p - z_s - \sum_{i=1}^{N_{\text{cheb}}} g_i T_i(z_s^*) \right). \quad (10)$$

Since we will include the g_i as additional parameters, with fiducial values $g_i = 0$, we shall need to take derivatives with one nonzero g_i at a time and therefore we can assume $\Delta(z_p - z, z_p) = \delta(z_p - z_s - g_i T_i(z_s^*))$ for a single i . Using the fact that $\delta(F(x)) = \sum 1/|F'(x_0)| \delta(x - x_0)$ for a function $F(z)$, where the sum runs over the roots of the equation $F(x) = 0$, and further using a recursive formula for the derivative of the Chebyshev polynomial (Arfken 2000, § 13.3), we get

$$n_p(z_p) = \sum_a \frac{n(z_a)}{\left| 1 + \frac{2g_i}{z_{\text{max}}[1 - (z_a^*)^2]} [-iz_a T_i(z_a^*) + iT_{i-1}(z_a^*)] \right|} \quad (11)$$

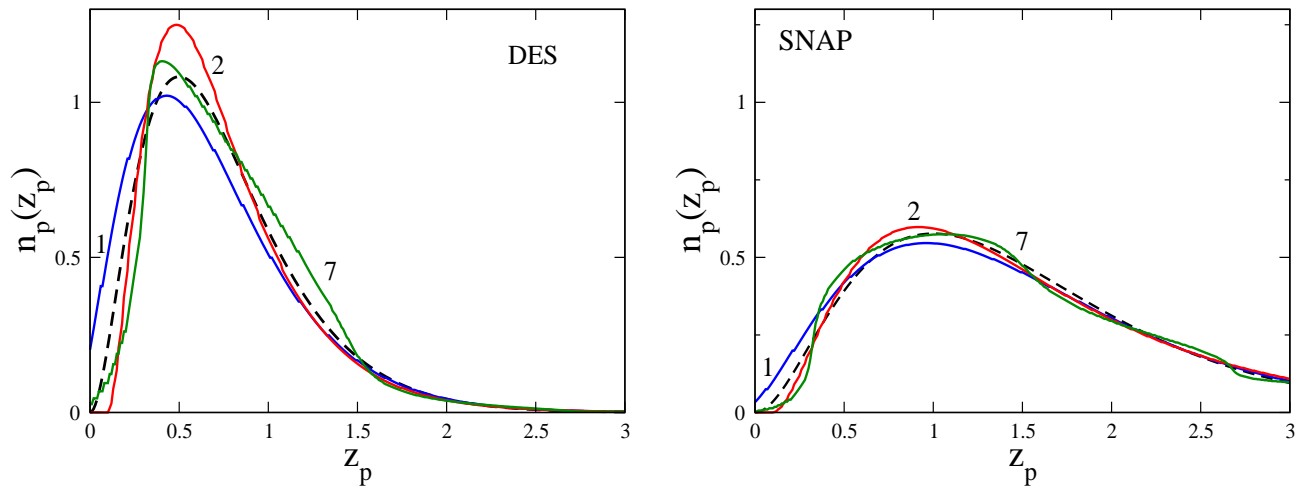


FIG. 1: Select three modes (first, second and seventh) of perturbation to the distribution of galaxies $n(z)$ for the DES (left) and SNAP (right), shown together with the original unperturbed distribution (dashed curve in each panel). These three modes correspond to the modes of perturbation in the $z_p - z_s$ relation shown in Fig. 9 in the Appendix. Note that SNAP’s fiducial $n(z)$ is broader, making the resulting wiggles in $n_p(z_p)$ less pronounced and the weak lensing measurements therefore less susceptible to the redshift biases. Note also that the allowed perturbations to $n(z)$ are not only located near the peak of the distribution, but can also have significant wiggles near the tails of the distribution.

where the sum runs over all roots of the equation $z + g_i T_i(z^*) - z_p = 0$, with (recall) $z_a^* \equiv (z_a - z_{\max}/2)/(z_{\max}/2)$. This is the expression for the perturbed distribution of galaxies due to a single perturbation mode.⁸ We use it, together with the original distribution $n(z)$, to compute the perturbed and unperturbed convergence power spectra and thus take the derivative with respect to g_i .

In Fig. 1 we show the photometric galaxy distributions $n_p(z_p)$ for the select three Chebyshev modes (first, second and seventh) of perturbation to the distribution of galaxies $n(z)$ corresponding to Fig. 9, together with the original unperturbed distribution. The distributions are shown for the DES and SNAP. Since the incorrect assignment of photometric redshifts only redistributes the galaxies, we always impose the requirement $\int_0^\infty n_p(z_p) dz_p = 1$ regardless of the perturbation. Note that SNAP’s fiducial $n(z)$ is broader, making the resulting wiggles in $n_p(z_p)$ less pronounced and helping the weak lensing measurements be less susceptible to the redshift biases. (As shown in § IV A, this effect is counteracted by the smaller fiducial errors in the SNAP survey which lead to more susceptibility to biases.)

B. Multiplicative errors

The multiplicative error in measuring shear can be generated by a variety of sources. For example, a circular PSF of finite size is convolved with the true image of the galaxy to produce the observed image, and in the process it introduces a multiplicative error. Let $\hat{\gamma}(z_s, \mathbf{n})$ and $\gamma(z_s, \mathbf{n})$ be the estimated and true shear of a galaxy at some true (spectroscopic) redshift z_s and direction \mathbf{n} . Then the general multiplicative factor $f_i(\theta)$ acts as

$$\hat{\gamma}(z_s, \mathbf{n}) = \gamma(z_s, \mathbf{n}) \times [1 + f_i(z_s, \mathbf{n})] \quad (12)$$

where f_i is the multiplicative error in shear which is both direction and time dependent. We can write the error as a sum of its mean (average over all directions and redshifts in that tomographic bin) and a component with zero mean,

$$f(z_{s,i}, \mathbf{n}) = f_i + r_i(\mathbf{n}) \quad (13)$$

⁸ Note that, for $g_i \ll 1$, Eq. (11) simplifies to $n_p(z_p) = n(z_p - g_i T_i(z_p^*))$

where $\langle f(z_{s,i}, \mathbf{n}) \rangle = f_i$ and $\langle r_i(\mathbf{n}) \rangle = 0$ and the averages are taken over angle and over redshift within the i th redshift bin. Then we can write

$$\langle \hat{\gamma}(z_{s,i}, \mathbf{n}) \hat{\gamma}(z_{s,j}, \mathbf{n} + d\mathbf{n}) \rangle = \langle \gamma(z_{s,i}, \mathbf{n}) \gamma(z_{s,j}, \mathbf{n} + d\mathbf{n}) (1 + f(z_{s,i}, \mathbf{n})) (1 + f(z_{s,j}, \mathbf{n})) \rangle \quad (14)$$

$$\simeq \langle \gamma(z_{s,i}, \mathbf{n}) \gamma(z_{s,j}, \mathbf{n} + d\mathbf{n}) \rangle (1 + f_i + f_j) \quad (15)$$

where we dropped terms of order $\langle \gamma \gamma f_i f_j \rangle$. Since the random component of the multiplicative error is uncorrelated with shear, all terms of the form $\langle \gamma \gamma r \rangle$ are zero. Finally, terms of the form $\langle \gamma \gamma r r \rangle$ are taken to be small, thus requiring that $\langle r_i(\mathbf{n}) r_j(\mathbf{n} + d\mathbf{n}) \rangle$ is smaller than f_i and f_j (Guzik and Bernstein, 2005). Therefore

$$\hat{P}_{ij}^\kappa(\ell) = P_{ij}^\kappa(\ell) \times [1 + f_i + f_j] \quad (16)$$

where again we emphasize that f_i is the irreducible part of the multiplicative error in i th redshift bin (i.e. its average over all directions *and* the i th redshift slab). It is clear that multiplicative errors are potentially dangerous, since they lead to an error that goes as f_i and not f_i^2 . Finally, note that shear calibration is likely to depend on the size of the galaxy, so that the mean error f_i is the error averaged over all galaxy sizes in bin i .

C. Additive errors

Additive error in shear is generated, for example, by the anisotropy of the PSF. We define the additive error via

$$\hat{\gamma}(z_s, \mathbf{n}) = \gamma(z_s, \mathbf{n}) + \gamma_{\text{add}}(z_s, \mathbf{n}) \quad (17)$$

Let us assume that the additive error is uncorrelated with the *true* shears so that the term $\langle \gamma(\mathbf{n}) \gamma_{\text{add}}(\mathbf{n}) \rangle$ is zero. Furthermore, let the Legendre transform of the term $\langle \gamma_{\text{add}}(\mathbf{n}) \gamma_{\text{add}}(\mathbf{n}) \rangle$ be $P_{\text{add}}^\kappa(\ell)$. Then we can write

$$\hat{P}_{ij}^\kappa(\ell) = P_{ij}^\kappa(\ell) + P_{\text{add}}^\kappa(\ell). \quad (18)$$

We now have to specify the additive systematic power $P_{\text{add}}^\kappa(\ell)$. Consider some known sources of additive error: for example, the additive error induced due to a non-circular PSF is roughly $R e_{\text{PSF}}$ where e_{PSF} is the ellipticity of the PSF and $R \equiv (s_{\text{PSF}}/s_{\text{gal}})^2$ is the ratio of squares of the PSF and galaxy size (E. Sheldon, private communication); galaxies that are smaller therefore have a larger additive error. Of course, the observer needs to correct the overall trend in the error, leaving only a smaller residual, and the impact of this residual is what we are interested in. It should be clear from this discussion that the additive error in shear can be calibrated by a part that depends on the average size of a galaxy at a given redshift multiplied by a random component that depends on the part of the sky observed. Therefore, we write the additive shear as $\gamma_{\text{add}}(z_{s,i}, \mathbf{n}) = b_i r(\mathbf{n})$ where b_i is the characteristic additive shear amplitude in the i th redshift bin and $r(\mathbf{n})$ is a random fluctuation.

In multipole space, the two point function can then be expressed as $b_i b_j$ times the angular part which only depends on $|\mathbf{n}_i - \mathbf{n}_j|$. Note that the additive error for two galaxies at different redshifts (i.e. when $i \neq j$) is not zero, although it may in principle be suppressed relative to the additive error for the auto-power spectra (when $i = j$). Motivated by such considerations, we assume the additive systematic in multipole space of the form

$$P_{\text{add},ij}^\kappa(\ell) = \rho b_i b_j \left(\frac{\ell}{\ell_*} \right)^\alpha \quad (19)$$

where the correlation coefficient ρ describes correlations between bins. The coefficient ρ is always set to unity for $i = j$, and for $i \neq j$ it is fixed to some fiducial value (not taken as a parameter in the Fisher matrix). While the discussion above would imply that $\rho = 1$ for all i and j , we allow for the possibility that the additive errors are not perfectly correlated across redshift bins. In the extreme case of uncorrelated additive errors in different z bins, the cross-power spectra are not affected, $\rho = \delta_{ij}$. We shall see that the results are weakly dependent on the fiducial value of ρ unless if $\rho = 1$ identically.

For the multipole dependence of P_{add}^κ we assume a power-law form, and marginalize over the index α . We choose $\ell_* = 1000$, near the ‘‘sweet spot’’ of weak lensing surveys, but note that this choice is arbitrary and made solely for our convenience since ℓ_* is degenerate with the parameters b_i . Our *a priori* expectation for the value of α is uncertain, and we try several possibilities but find (as discussed later) that the results are insensitive to the value of α . We therefore have a total of $B + 1$ nuisance parameters for the additive error (B parameters b_i , plus α).

In practice there is no particular reason why an additive systematic would be expected to conform to a power law, so in the future we should consider an additive systematic with more freedom in its spatial behavior. The current treatment is optimistic: fixing the systematic to a power law gives it an identifying characteristic that allows us to distinguish it from cosmological signals. Without such a characteristic, the systematic could be much more damaging.

D. Putting the systematics together

With the systematic errors we consider, the resulting theoretical convergence power spectrum is

$$\hat{P}_{ij}^{\kappa}(\ell) \equiv \hat{P}^{\kappa}(\ell, z_s^{(i)}, z_s^{(j)}) = P^{\kappa}(\ell, z_s^{(i)} + \delta z_p^{(i)}, z_s^{(j)} + \delta z_p^{(j)}) \times [1 + f_i + f_j] + \rho b_i b_j \left(\frac{\ell}{\ell_*}\right)^{\alpha}. \quad (20)$$

The derivatives with respect to the multiplicative and additive parameters are trivial since they enter as linear (or power-law) coefficients, while the derivatives with respect to the redshift parameters $\delta z_p^{(k)}$ (really, parameters g_i defined in Eq. (7)) need to be taken numerically.

IV. RESULTS: REDSHIFT SYSTEMATICS

A. Centroids of redshift bins

We have a total of $N + B$ parameters, and we marginalize over the B redshift bin centroids by giving them identical Gaussian priors. While the actual redshift accuracy may be better in some redshift ranges than in others, the required accuracy that we obtain in our approach will pertain to the redshift bins where observations are most sensitive (i.e. at intermediate redshifts $z \sim 0.5 - 1$).

Figure 2 shows the degradation in Ω_M , σ_8 and $w = \text{const}$, and also w_0 and w_a , accuracies as a function of our prior knowledge of the redshift bin centroids. Here and in the subsequent two Figures, the plots are shown separately for each of the three surveys (DES, SNAP and LSST). Since we are using the Fisher matrix formalism without external priors on cosmological parameters, the cosmological parameter degradations (as well as accuracies) clearly remain unchanged for an arbitrary f_{sky} if we also scale the priors on the nuisance parameters by $f_{\text{sky}}^{-1/2}$. In these and subsequent plots we show the degradations for fiducial values of the sky coverage for each survey $f_{\text{sky, fid}}$, where $f_{\text{sky, fid}} = f_{5000}$, f_{1000} and f_{15000} for DES, SNAP and LSST respectively, while indicating that the requirements scale as $(f_{\text{sky}}/f_{\text{sky, fid}})^{-1/2}$.

We generally find that the degradations in different cosmological parameters are comparable. To have less than $\sim 50\%$ degradation, for example, we need to control the redshift centroid bias to about $0.003 (f_{\text{sky}}/f_{\text{sky, fid}})^{-1/2}$ for the DES and SNAP and to about $0.0015 (f_{\text{sky}}/f_{\text{sky, fid}})^{-1/2}$ for the LSST. The current statistical accuracy in *individual* galaxy redshifts is of order 0.02-0.05. Averaging the large number of galaxies in a given redshift bin, it may be that we are already close to the aforementioned requirement on the centroid bias, but this will of course depend on the control of systematics in the photometric procedure.

As mentioned in the Introduction, the accurately determined combination of w_0 and w_a , $F(w_0, w_a)$, is degraded in nearly the same way as constant w ; this is illustrated by a thick dashed line in each panel of Fig. 2. In the rest of the paper we do not repeat plotting the curves corresponding to $F(w_0, w_a)$ which nearly overlap those corresponding to $w = \text{const}$. Finally, we show the degradations for w_0 and w_a separately. Since these two parameters are determined to a substantially lower accuracy than $w = \text{const}$ (see Table II), it is not surprising that the degradations in these two are substantially smaller.

B. Chebyshev expansion in $z_p - z_s$

Figure 3 shows the degradation in the Ω_M , σ_8 and w , and also w_0 and w_a , as we marginalize over a large number ($N_{\text{cheb}} = 30$) of Chebyshev coefficients f_i each with the given prior. We checked that, when only $N \lesssim 5$ modes are allowed to vary, all parameters f_i can be self-consistently solved from the survey – this is an example of self-calibration. However, with a larger number of Chebyshev modes the self-calibration regime is lost. Since we are interested in the most general form of the redshift bias, this is the regime we would like to explore. We have also checked that, as we let the number of coefficients increase further, the errors in cosmological parameters do not increase indefinitely, as the rapid fluctuations in the $z_p - z_s$ are not degenerate with cosmology. In fact we found that the degradations have

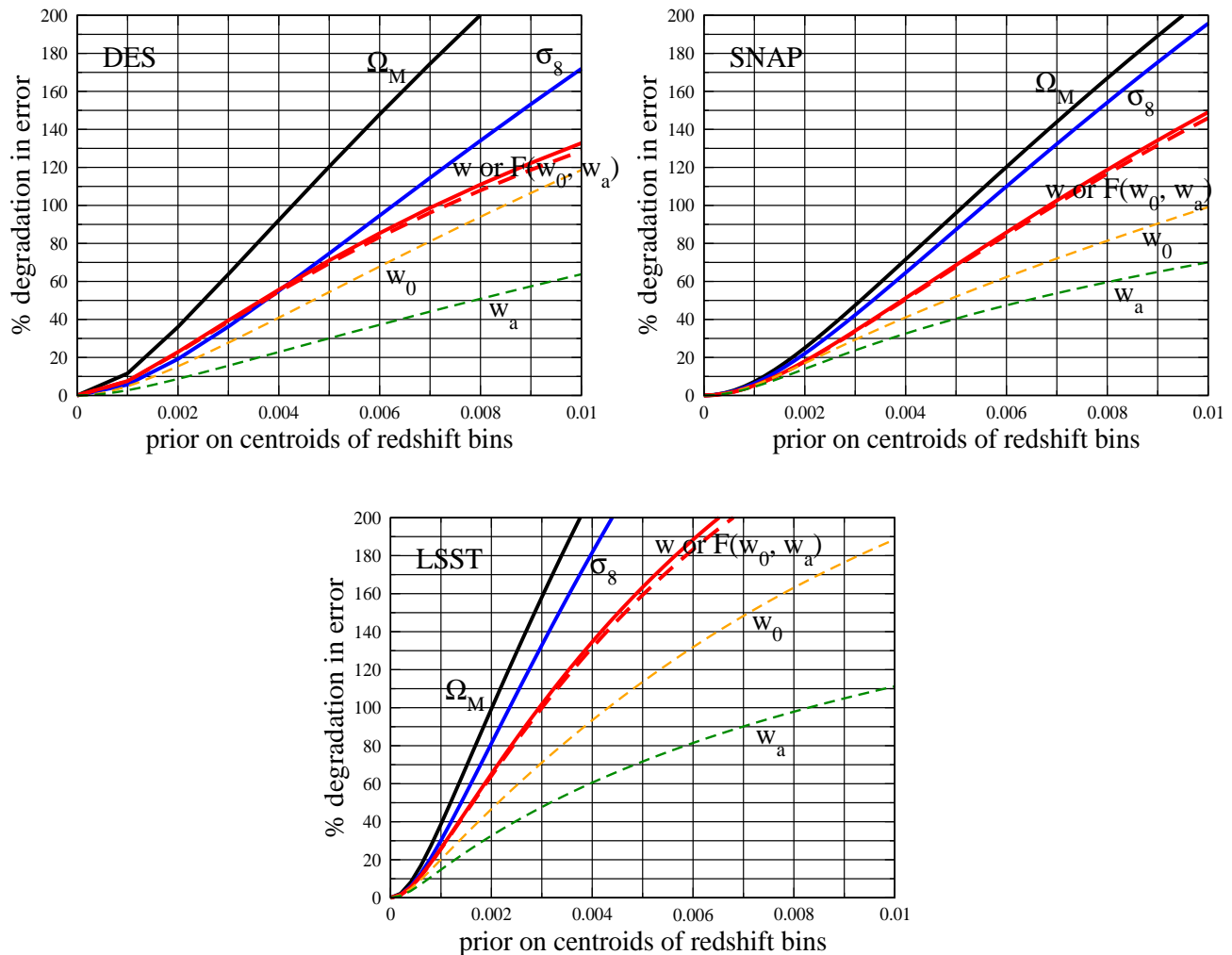


FIG. 2: Degradation in the cosmological parameter accuracies as a function of our prior knowledge of $\delta z \equiv z_p - z_s$. We assume equal Gaussian priors to each redshift bin centroid, shown on the x-axis. For example, to have less than $\sim 50\%$ degradation in Ω_M , σ_8 or w , we need to control the redshift bias to about 0.003 $(f_{\text{sky}}/f_{\text{sky, fid}})^{-1/2}$ or better for the DES and SNAP, and to about 0.0015 $(f_{\text{sky}}/f_{\text{sky, fid}})^{-1/2}$ or better for the LSST. For the varying equation of state parameterization, the requirements for the best measured combination of w_0 and w_a ($F(w_0, w_a)$) are identical to those for $w = \text{const}$, while the requirements on w_0 and w_a individually are somewhat less stringent.

asymptoted to their final values once we include 20-30 Chebyshev polynomials; therefore, fluctuations in redshift on scales smaller than $\Delta z \sim 0.1$ are not degenerate with cosmological parameters. The choice of $N_{\text{cheb}} = 30$ coefficients is therefore conservative.

Figure 3 shows that the photometric redshift bias in each Chebyshev mode, for the DES and SNAP, should be controlled to about 0.001 $(f_{\text{sky}}/f_{\text{sky, fid}})^{-1/2}$ or less. For LSST, the requirement is more severe and we could tolerate biases no larger than about 0.0005 $(f_{\text{sky}}/f_{\text{sky, fid}})^{-1/2}$. These are fairly stringent requirements, in rough agreement with results found by Ma, Hu & Huterer (2005).

It might seem a bit surprising that the SNAP and DES requirements are comparable, given that the fiducial SNAP survey is more powerful than the DES (see Table II) and hence would need better control of the systematics. However, there is another effect at play here: a narrow distribution of galaxies in redshift, such as that from the DES, is more strongly subjected to fluctuations in $z_p - z_s$ than a wide distribution, such as that from SNAP; see Fig. 1. Therefore, surveys with wide leverage in redshift have an advantage in beating down the effect of redshift error, just as in the case of cluster count surveys (Huterer et al. 2004).

We now confirm the results by computing the bias in the cosmological parameters due to the bias in one of the

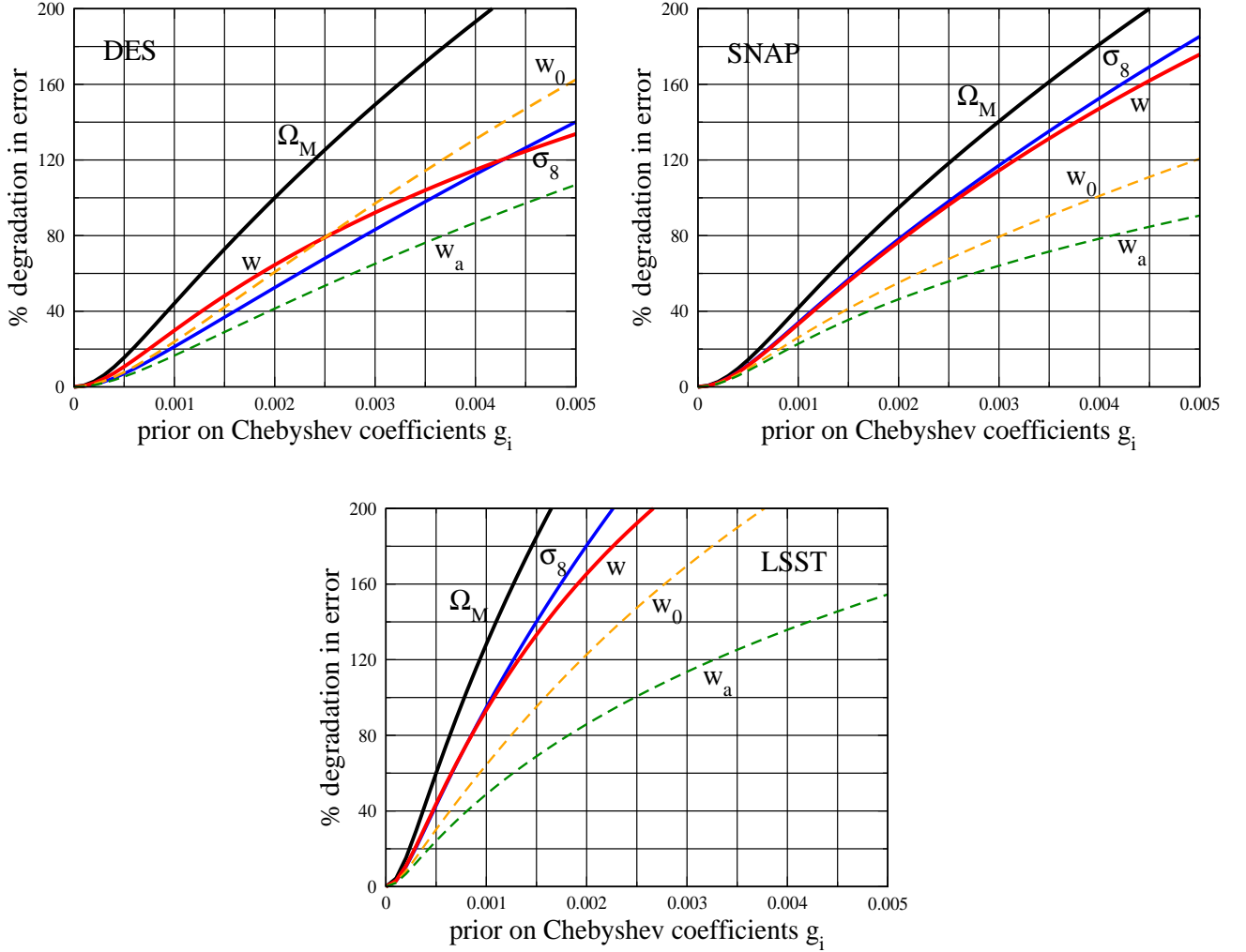


FIG. 3: Degradation in marginalized errors in Ω_M , σ_8 and $w = \text{const}$, as well as w_0 and w_a , as a function of our prior knowledge of the redshift bias coefficients f_i for the DES, SNAP and LSST. We use $N_{\text{cheb}} = 30$ parameters f_i that describe the bias in redshift and give equal prior to each of them, shown on the x-axis. For the DES and SNAP, knowledge of f_i to better than 0.001 $(f_{\text{sky}}/f_{\text{sky, fid}})^{-1/2}$, corresponding to redshift bias of $|z_p - z_s| \lesssim 0.001 (f_{\text{sky}}/f_{\text{sky, fid}})^{-1/2}$ for each Chebyshev mode, is desired as it leads to error degradations of about 50% or less. For LSST the requirement is about a factor of two stronger. These results are corroborated by computing the bias in cosmological parameters as discussed in the text.

redshift bias coefficients, dg_i . The bias in the cosmological parameter p_α can be computed as

$$\delta p_\alpha = F_{\alpha\beta}^{-1} \sum_{\ell} [C_i^\kappa(\ell) - \bar{C}_i^\kappa(\ell)] \text{Cov}^{-1} [\bar{C}_i^\kappa(\ell), \bar{C}_j^\kappa(\ell)] \frac{\partial \bar{C}_j^\kappa(\ell)}{\partial p_\beta} \quad (21)$$

where the summations over β , i and j were implicitly assumed and the covariance of the cross power spectra is given in Eq. (6). The source of the bias in the observed shear covariance, $C_i^\kappa(\ell) - \bar{C}_i^\kappa(\ell)$, is assumed to be the excursion of $dg_m = 0.001$ in the m th coefficient of the Chebyshev expansion, others being held to their fiducial values of zero. We then compare this error to the $1\text{-}\sigma$ marginalized error on the parameter p_α . For a range of $1 \leq m \leq 30$ we find that the biases in the cosmological parameters are entirely consistent with statistical degradations shown in Fig. 3. We also find that the degradations due to higher modes ($m \gtrsim 10\text{-}20$) are progressively suppressed, illustrating again that smooth biases in redshift are most important source of degeneracy with cosmological parameters, and need the most attention when calibrating the photometric redshifts.

Finally, let us note that in this analysis we have not attempted to model more complicated redshift dependences of bias, the presence of abrupt degradations in redshift etc. Such an analysis is beyond the scope of this work, but can

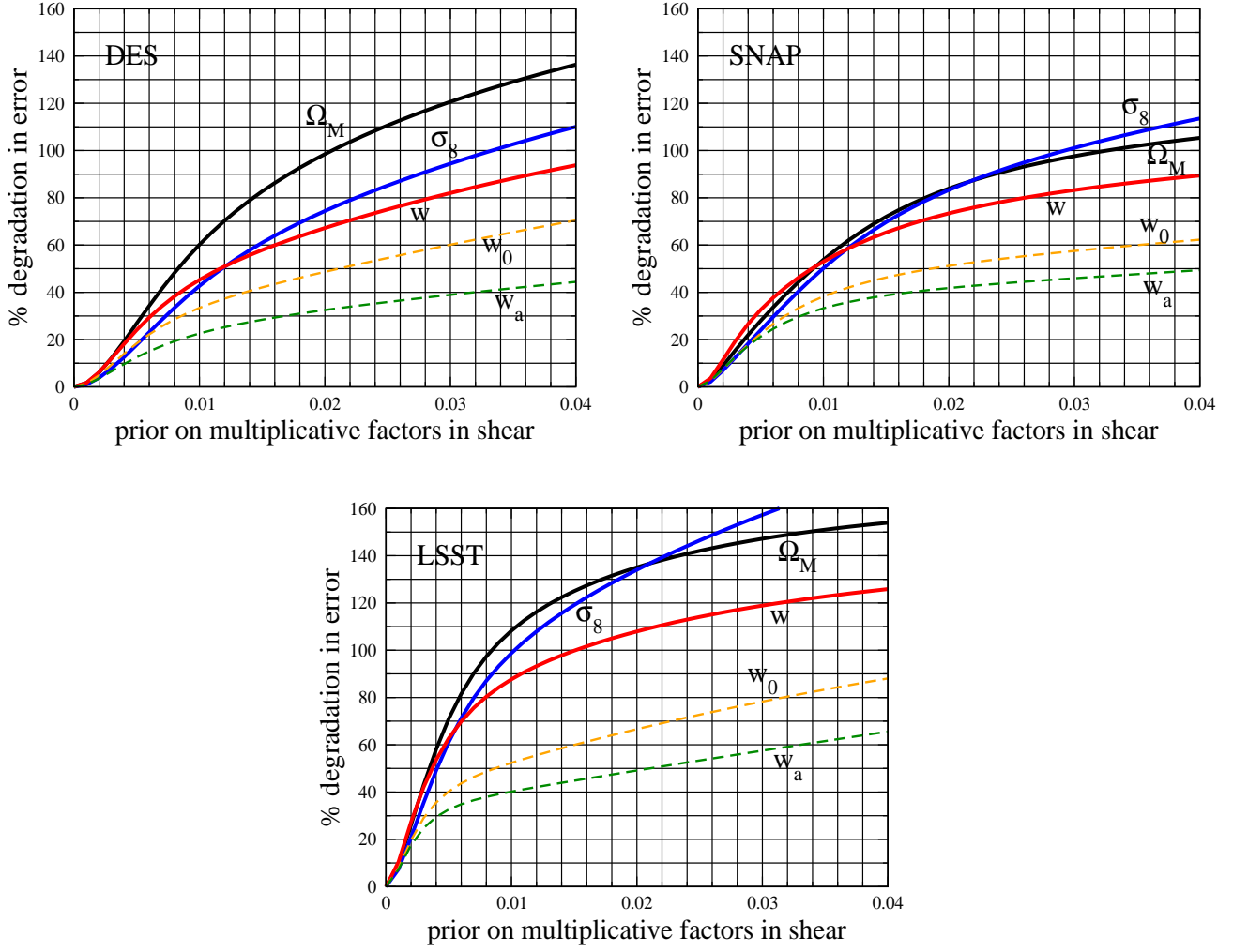


FIG. 4: Degradation in marginalized errors in Ω_M , σ_8 and $w = \text{const}$, as well as w_0 and w_a , as a function of our prior knowledge of the shear multiplicative factors. We give equal prior to multiplicative factors in all redshift bins, and show results for the DES, SNAP and LSST. For example, existence of the multiplicative error of 0.01 ($f_{\text{sky}}/f_{\text{sky, fid}})^{-1/2}$ (or 1% in shear for the fiducial sky coverages) in each redshift bin leads to 50% increase in error bars on Ω_M , σ_8 and w for the DES and SNAP, and about a 100% degradation for LSST.

be done using similar tools once the details about the performance of a given photometric method are known.

V. RESULTS – MULTIPLICATIVE ERROR

As explained in § III B, we adopt the multiplicative error of the form

$$\hat{P}_{ij}^{\kappa}(\ell) = P_{ij}^{\kappa}(\ell) \times [1 + f_i + f_j], \quad (22)$$

where $\hat{P}_{ij}^{\kappa}(\ell)$ and $P_{ij}^{\kappa}(\ell)$ are estimated and true convergence power respectively. In other words, the multiplicative error we consider can be thought of as an irreducible but perfectly coherent bias in the calibration of shear in any given redshift bin.

First, note that a tomographic measurement with B redshift bins can determine at most B multiplicative parameters f_i (this is true either if they are just stepwise excursions as assumed here or coefficients of Chebyshev polynomials described in the Appendix). For, if we had more than B multiplicative parameters, at least one bin would have

two or more parameters, and there would be an infinite degeneracy between them. In contrast, the survey can in principle determine a much larger number of cosmological parameters since they enter the observables in a more complicated way. We choose to use exactly $N_{\text{mult}} = B$ multiplicative parameters (so $N_{\text{mult}} = 10$ for SNAP and LSST and $N_{\text{mult}} = 7$ for the DES) since we would expect the shear calibration to be different within each redshift bin.

Figure 4 shows the degradation in error in measuring three cosmological parameters as a function of our prior knowledge of the multiplicative factors; we give equal prior to all multiplicative factors. For the DES and SNAP, control of multiplicative error of $0.01 (f_{\text{sky}}/f_{\text{sky, fid}})^{-1/2}$ (or 1% in shear for the fiducial sky coverages) leads to a 50% increase in the cosmological error bars, and is therefore about the largest error tolerable. For LSST, the requirement is about a factor of two more stringent.

In general, it is interesting to consider whether the weak lensing survey can ‘self-calibrate’, i.e. determine both the cosmological and the nuisance parameters concurrently. This is partly motivated by the self-calibration of cluster count surveys, where it has been shown that one can determine the cosmological parameters and the evolution of the mass-observable relation – provided that the latter takes a relatively simple deterministic form (e.g. Levine, Schulz & White 2002, Majumdar & Mohr 2003, Hu 2003b, Lima & Hu 2004). Figure 4 shows that the fiducial DES and SNAP surveys can self-calibrate with about a 100% degradation in cosmological parameter errors (and LSST with about a 150% degradation). While doubling the error in cosmological parameters is a somewhat steep price to pay, it is very encouraging that all surveys enter a self-calibrating regime where only the higher-order moments of the error contribute to the total error budget. In § VII we show that the inclusion of bispectrum information can significantly improve the self-calibration regime.

VI. RESULTS: ADDITIVE ERROR

As explained in § III C, we adopt the additive error of the form

$$P_{\text{add},ij}^{\kappa}(\ell) = \rho b_i b_j \left(\frac{\ell}{\ell_*} \right)^{\alpha}, \quad (23)$$

which adds that amount of noise to the convergence power spectra. The coefficient ρ is always 1 for $i = j$, and its (fixed) value for $i \neq j$ controls how much additive error leaks into the cross power spectra. We weigh the fiducial value of b_i by the inverse square of the average galaxy size in i th redshift bin (or, by the square of the angular diameter distance to the i th bin)⁹.

Figure 5 shows the degradations in the equation of state w as a function of the fiducial b_i at redshift $z = 0.75$ where, very roughly, most galaxies are found (recall, the other b_i are equal to this value modulo order-unity weighting by the square of the angular diameter distance to their corresponding redshift). The solid line in the figure shows results for our fiducial SNAP survey, assuming no contribution to the cross-power spectra (i.e. $\rho = \delta_{ij}$). The coefficients b_i need to be controlled to $\sim 2 \times 10^{-5}$, corresponding to shear variance of $\ell(\ell+1)P_{\text{add},ij}^{\kappa}(\ell)/(2\pi) \sim 10^{-4}$ on scales of ~ 10 arcmin ($\ell \sim 1000$) where most constraining power of weak lensing resides. The observed degradation in cosmological parameters is clearly due to the increased sample variance that the additional power puts onto the measurement of the power spectrum. When $\rho = 1$, this sample variance is confined to a single mode of the shear covariance matrix, so that the maximum damage is limited and we observe the self-calibration plateau in Fig. 5.¹⁰

We have tried varying a number of other details:

- Using different values of the coefficient ρ for $i \neq j$ in the range $0 \leq \rho < 1$.
- Changing the fiducial value of the exponent α from 0 to +3 or −3.
- Adding a 10% prior to the b_i (rather than no prior).
- Using the redshift independent fiducial values of the coefficients b_i .
- Considering the degradation in the other cosmological parameters.

⁹ For $b_i = 0$, the Fisher derivatives with respect to b_i are zero and no information about these parameters can formally be extracted.

¹⁰ One could in principle also have a worst-case limit with additive errors whose functional form makes them strongly degenerate with the effect of varying the cosmological parameters, where the accuracy in cosmological constraints degrades as soon as the additive power becomes comparable to the *measurement uncertainties* in the power spectrum (and not the power spectrum itself, as above).

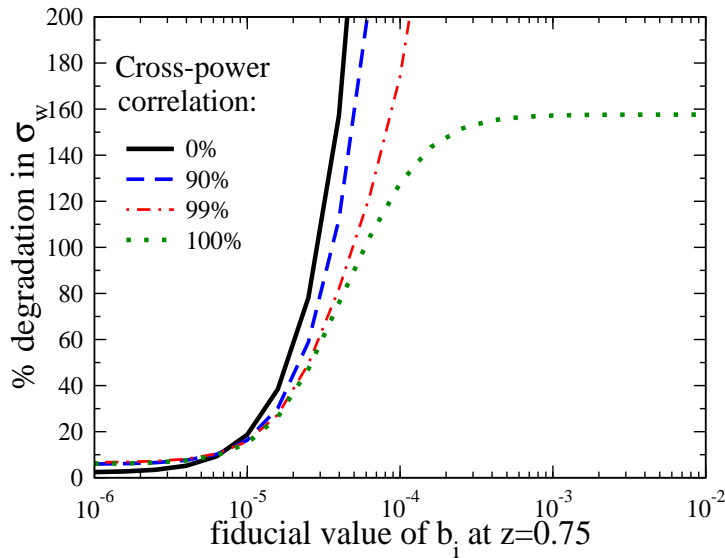


FIG. 5: Degradation in the cosmological parameter accuracies as a function of the *fiducial value* of the additive shear errors b_i , assuming no prior on the b_i . We show results for SNAP and for several values of the correlation coefficients between different bins, ρ , and marginalizing over the spatial power law exponent α which has fiducial value $\alpha = 0$. The results are insensitive to various details, as discussed in the text, and the only exception is the possibility that the additive effect on the cross-power spectra is negligibly suppressed (i.e. that the cross-power correlation is close to 100%). We conclude that the mean additive shear will need to be known to about $\sim 2 \times 10^{-5}$, corresponding to shear variance of $\sim 10^{-4}$ on scales of ~ 10 arcmin.

Interestingly, we find that the overall requirements are very weakly dependent on any of the above variations, and the requirements almost always look roughly like those in Figure 5. In particular, the results are essentially insensitive to reasonable priors of any of the nuisance parameters, since the b_i can be determined internally to an accuracy much better than b_i for all but the smallest ($\lesssim 10^{-7}$) fiducial values of these parameters. Therefore the dominant effect by far is the fiducial value of b_i and the increased sample variance that it introduces.

The only interesting exception to this insensitivity is allowing the $i \neq j$ value of the coefficients ρ to be very close to unity. In the extreme case when $\rho = 1$ for $i \neq j$, the degradation asymptotes to $\sim 150\%$ even with very large b_i since in that case the additive errors add a huge contribution to *all* power spectra, and one can mathematically show that the resulting errors in cosmological parameters do not change more than $\sim 100\%$ irrespective of the systematic error. In practice, however, $\rho \gtrsim 0.99$ for $i \neq j$ is needed to see an appreciable difference (see the other curves in Fig. 5), and it is reasonable to believe that the actual errors in the cross-power spectra will be suppressed by much more than a percent, resulting in the degradations as shown by the solid curve in Fig. 5.

While our model for the additive errors is admittedly crude, it is very difficult to parameterize these errors more accurately without end-to-end simulations that describe various systematic effects and estimate their contribution to the additive errors (such simulations are now being planned or carried out by several research groups). Moreover, additive errors cannot be self-calibrated unless we can identify a functional dependence, which is distinct from the cosmological dependence of the power spectrum, that it must have. Finally, we note that space-based surveys, such as SNAP, are expected to have a more accurate characterization of the additive error, primarily from the absence of atmospheric effects in the characterization of the PSF.

VII. SYSTEMATICS WITH THE BISPECTRUM

We now extend the calculations to the bispectrum of weak gravitational lensing. The bispectrum is the Fourier counterpart of the three-point correlation function, and it describes the non-Gaussianity of mass distribution in the large-scale structure that is induced by gravitational instability from the primordial Gaussian perturbations that the simplest inflationary models predict. The redshift evolution and configuration dependence of the mass bispectrum can be accurately predicted using a suite of high-resolution N -body simulations (see e.g. Bernardeau et al. 2002 for a comprehensive review). The bispectrum of lensing shear arises from the line-of-sight integration of products of the mass bispectrum and the lensing geometrical factor (see Eq. (18) in Takada & Jain 2004). Following Jain & Seljak

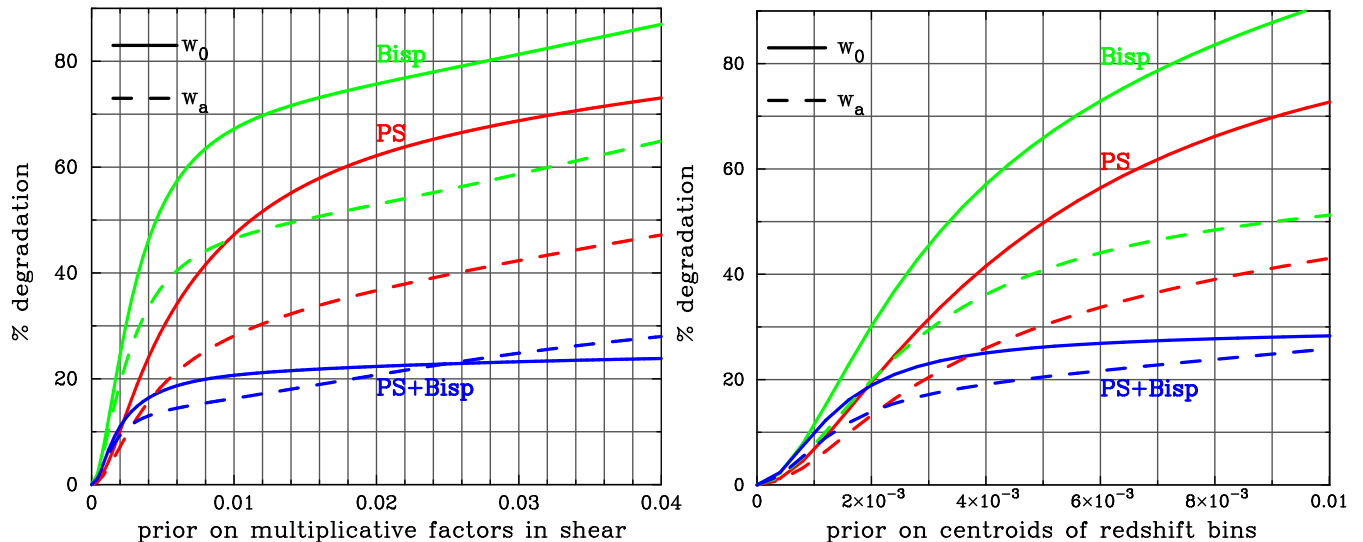


FIG. 6: Degradation in w_0 and w_a accuracies expected for the SNAP as a function of our prior knowledge of the multiplicative error in shear (left panel) and redshift centroids (right panel). The priors on the multiplicative or redshift parameters are shown on the x-axis. While the power spectrum (PS) and bispectrum (BS) individually enter a self-calibration regime with $\sim 100\%$ degradation in cosmological parameter errors, combining the two leads to self-calibration with only a 20-30% degradation. This improvement in the self-calibration limit is in addition to the already smaller no-systematic error bars with PS+BS as compared to either PS or BS alone.

(1997), we roughly estimate how the lensing power spectrum and bispectrum scale with cosmological parameters by perturbing around the fiducial Λ CDM model:

$$P^\kappa \propto \Omega_{\text{DE}}^{-3.5} \sigma_8^{2.9} z_s^{1.6} |w|^{0.31}, \quad B^\kappa \propto \Omega_{\text{DE}}^{-6.1} \sigma_8^{5.9} z_s^{1.6} |w|^{0.19}, \quad (24)$$

where we have considered multipole mode of $l = 1000$, equilateral triangle configurations in multipole space, redshift of all source galaxies $z_s = 1$ (no tomography), and constant equation of state parameter w . We adopt the model described in Takada & Jain (2004) to compute the lensing bispectrum. Equation (24) illustrates that the power spectrum and the bispectrum depend upon specific combinations of cosmological parameters. For example, the power spectrum (and more generally any two-point statistics of choice) depends on Ω_{DE} and σ_8 through the combination $\Omega_{\text{DE}}^{-1.2} \sigma_8$ (or equivalently $\Omega_M^{0.5} \sigma_8$). Furthermore, the cosmological parameter dependences are strongly degenerate with source redshift (z_s) unless accurate redshift information is available. Importantly, the power spectrum and bispectrum have substantially *different* dependences on the parameters, suggesting that combining the two can be a powerful way of breaking the parameter degeneracies. For example, it is well known that a combination of B/P^2 , motivated from the hierarchical clustering ansatz, depends mainly on Ω_{DE} , with rather weak dependence on σ_8 , so that roughly $B/P^2 \propto \Omega_{\text{DE}}^{0.9} \sigma_8^{-0.1}$ (Bernardeau et al. 1997, Hui 1999, Takada & Jain 2004). As another example, the bispectrum amplitude increases with the mean source redshift z_s more slowly than P^2 because the non-Gaussianity of structure formation becomes suppressed at higher redshifts. It is therefore clear that photometric redshift errors of source galaxies will affect the power spectrum (PS) and bispectrum (BS) differently. Likewise, it is natural to expect that other systematics that we have considered affect the power spectrum and the bispectrum in a different way.

For the PS+BS systematic analysis, we consider the redshift and multiplicative errors but not the additives. For the redshift errors we adopt the parameterization of redshift bin centroids, now applied to tomographic bins of both PS and BS. The multiplicative error is modeled similarly as in §III B: the observed bispectrum with tomographic redshift bins i, j and k , $\hat{B}_{ijk}(l_1, l_2, l_3)$, is related to the true bispectrum $B_{ijk}(l_1, l_2, l_3)$ via

$$\hat{B}_{ijk}(l_1, l_2, l_3) = B_{ijk}(l_1, l_2, l_3) \times [1 + f_i + f_j + f_k]. \quad (25)$$

Based on the considerations above, we study how combining the power spectrum with the bispectrum allows us to break parameter degeneracies not only in cosmological parameter space but also those induced by the presence of the nuisance systematic parameters. We include all triangle configurations, and compute the bispectra constructed using 5 redshift bins up to $l_{\text{max}} = 3000$. Note that, for a given triangle configuration, there are 5^3 tomographic bispectra; the large amount of time necessary to compute them is the reason why we use 5 tomographic bins instead

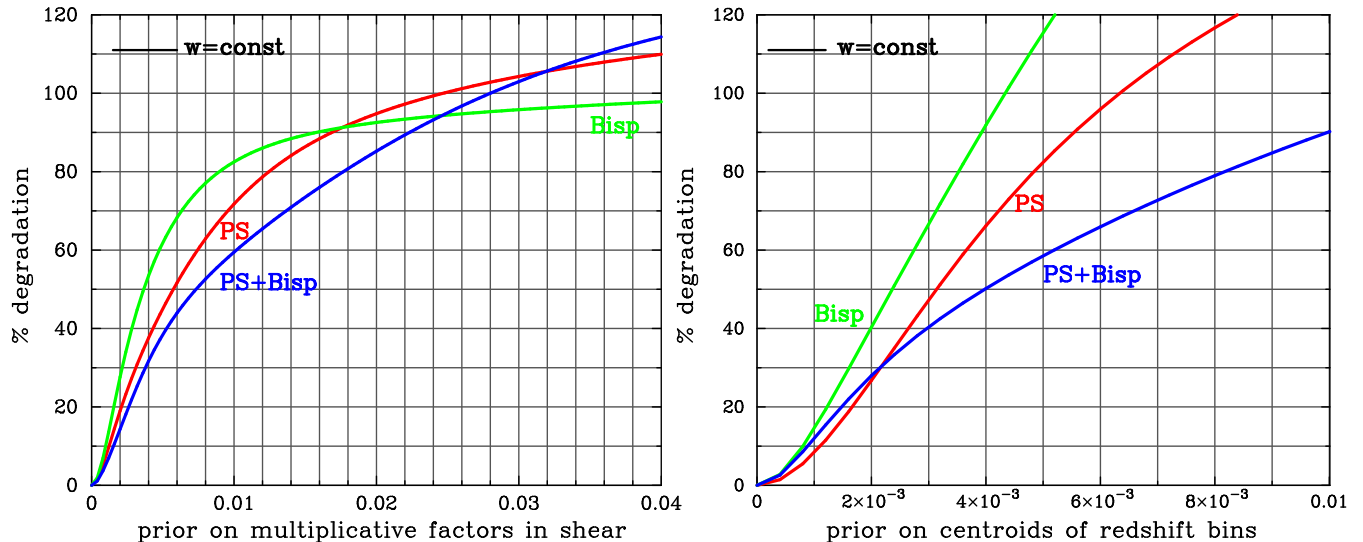


FIG. 7: Degradation in $w = \text{const}$ for the multiplicative errors (left panel) and redshift errors (right panel). Note that the low self-calibration asymptote seen in Fig. 6 is not seen any more, and even the cases when PS+BS are combined lead to appreciable degradations. We conclude that $w = \text{const}$ (or more generally any accurately measured combination of $w(z)$) does not benefit from self-calibration much, but w_0 and w_a individually do as shown in Fig. 6.

of the original 7-10.¹¹ Note too that we have assumed that the PS and BS are uncorrelated and simply added their Fisher matrices when combining them. While they are strictly uncorrelated in linear theory, nonlinear structure formation will introduce the correlation between the two, and the full information content will be smaller than our estimate¹². Correlation between the PS and BS has not been accurately estimated to date, and such a project is well beyond the scope of our paper. However, our main emphasis here is not to accurately estimate the resulting cosmological error bars but rather to study the overall effect of the systematics when different weak lensing probes are combined. We expect the qualitative trends (discussed below) to be unchanged in cases when we add information from cross-correlation cosmography or cluster counts to the PS.

Figure 6 shows how the multiplicative errors (left panel) and redshift centroid errors (right panel) degrade constraints on w_0 and w_a expected for SNAP. Each panel shows the degradation in the parameter measurement due to the power spectrum, bispectrum, and the two combined. The most remarkable fact seen in Fig. 6 is that the *degradation* in the parameter accuracies is smaller with PS and BS combined as opposed to either one separately. This is because dependences of BS on cosmological parameters as well as the model systematics are complementary to those from PS. Therefore, combining the PS and BS has a very beneficial effect of protecting against the systematics by more than a factor of two than either statistic alone!

However, the drastic improvement in self-calibration does not hold up for parameters that are more accurately measured, such as $w = \text{const}$. Figure 7 shows the degradation in the $w = \text{const}$ case for the multiplicative errors (left panel) and redshift errors (right panel). It is clear that the low self-calibration asymptote seen in Fig. 6 is no longer present, and even the cases when PS and BS are combined lead to appreciable degradations. Therefore, $w = \text{const}$ does not benefit from self-calibration as much as w_0 and w_a . More generally, self-calibration with PS+BS works much better when applied to poorly determined combinations of cosmological parameters than to the accurately determined ones; we have explicitly checked this by diagonalizing the full Fisher matrix and finding the degradations in all of its eigenvectors.

VIII. COMBINING THE SYSTEMATIC ERRORS

In Table II we now show the principal cosmological parameter with their fiducial values, and their errors for the PS only and PS+BS cases. In each case we show the error without any systematics, and the error after adding sample

¹¹ For the same reason, the PS curves in Figs. 6 and 7 do not exactly match those in Figs. 2 and 4.

¹² We thank Martin White for drawing our attention to this issue.

Parameter	Fiducial value	DES (PS)	DES (PS+BS)	SNAP (PS)	SNAP (PS+BS)	LSST (PS)	LSST (PS+BS)
Ω_M	0.3	0.008/0.011	0.006/0.009	0.008/0.011	0.004/0.006	0.003/0.007	0.002/0.005
w	-1.0	0.092/0.120	0.035/0.060	0.058/0.081	0.027/0.036	0.029/0.053	0.010/0.023
σ_8	0.9	0.010/0.012	0.006/0.008	0.008/0.011	0.005/0.008	0.004/0.006	0.003/0.004
w_0	-1.0	0.33/0.40	0.18/0.20	0.28/0.35	0.09/0.12	0.13/0.20	0.06/0.07
w_a	0	1.41/1.64	0.82/0.92	0.96/1.20	0.35/0.44	0.49/0.69	0.25/0.27

TABLE II: Cosmological parameter errors without the systematics (numbers preceding the slash in each box) and with sample systematics (numbers following the slash). For the systematics case we assumed redshift biases (described by Chebyshev polynomials) of 0.0005, *together with* the multiplicative errors of 0.005. The errors are shown for the power spectrum tomography only (PS), and for the power spectrum and the bispectrum (PS+BS). Errors in other cosmological parameters ($\Omega_M h^2$, $\Omega_B h^2$, n) are not shown.

systematic errors. For the systematics, we assume redshift biases (described by Chebyshev polynomials) with priors of 0.0005, *together with* the multiplicative errors of 0.005. The errors have been marginalized over the other cosmological parameters, and the systematic-case errors have further been marginalized over the 30 redshift and 10 multiplicative nuisance parameters with the aforementioned priors. While the systematics used are a guess – and they are likely to remain uncertain well into the planning phase of each survey – our goal here is to see how the errors degrade. While the errors in the strongest fiducial surveys get degraded the most, we find that strongest surveys remain in that position even after adding the systematics. For example, LSST’s fiducial error on w was a factor of two better than SNAP’s before adding the systematics, and is 50% better after adding them. Note, however, that we have added *equal* systematic errors to all three surveys in this example; in reality, a space-based survey like SNAP is expected to have a better control of the systematics than the ground based surveys (see e.g. Rhodes et al. 2004).

In Fig. 8 we show the contours of constant degradation in equation of state of dark energy w (for the PS case only) with both redshift and multiplicative errors included. The x and y-axis intercepts of degradation values in this Figure correspond to the case of redshift centroid errors only (as in Fig. 2) and multiplicative errors only (as in Fig. 4) respectively, but the rest of the plane allows for the simultaneous presence of both types of error. Note that the contours become progressively more vertical at larger values of the redshift error – therefore, the results are weakly affected by the multiplicative errors once the redshift errors become substantial. However, we would ideally like to be in the regime where the degradation is smaller than $\sim 50\%$, and in that case both types of error (as well as the additives) need to be controlled to a correspondingly good accuracy as discussed in § IV A and § V.

IX. CONCLUSIONS

We considered three generic types of systematic errors that can affect a weak lensing survey: measurements of source galaxy redshifts, and multiplicative and additive errors in the measurements of shear. We considered three representative future wide-field surveys (DES, SNAP and LSST) and used weak lensing tomography with either power spectrum alone, or power spectrum and bispectrum combined.

The most important (and difficult) part is to parameterize the systematic errors. We are solely interested in the part of the systematics that has not been corrected for in the data analysis, as that part can lead to errors in the estimated cosmological parameters. For the redshift error we adopt two alternative parameterizations that should both be useful in calibrating photometric redshift methods. Multiplicative errors in shear measurement are described by one parameter for the error in shear in each given redshift bin. The additive errors are most difficult to parameterize, as their redshift dependence and spatial coherence both need to be specified; our treatment of the additive errors, while robust with respect to various details of the model, is only a first step and can be improved upon with further simulation of realistic systematics.

In general, higher fiducial accuracy in the cosmological parameters leads to more stringent requirements on the systematics. Therefore, LSST typically has the most stringent requirements, followed by SNAP and then the DES (at their fiducial f_{sky}). We note that the *accurately determined* combinations of dark energy parameters typically are more sensitive to systematics than the *poorly determined* combinations. At this point one could ask, which is the

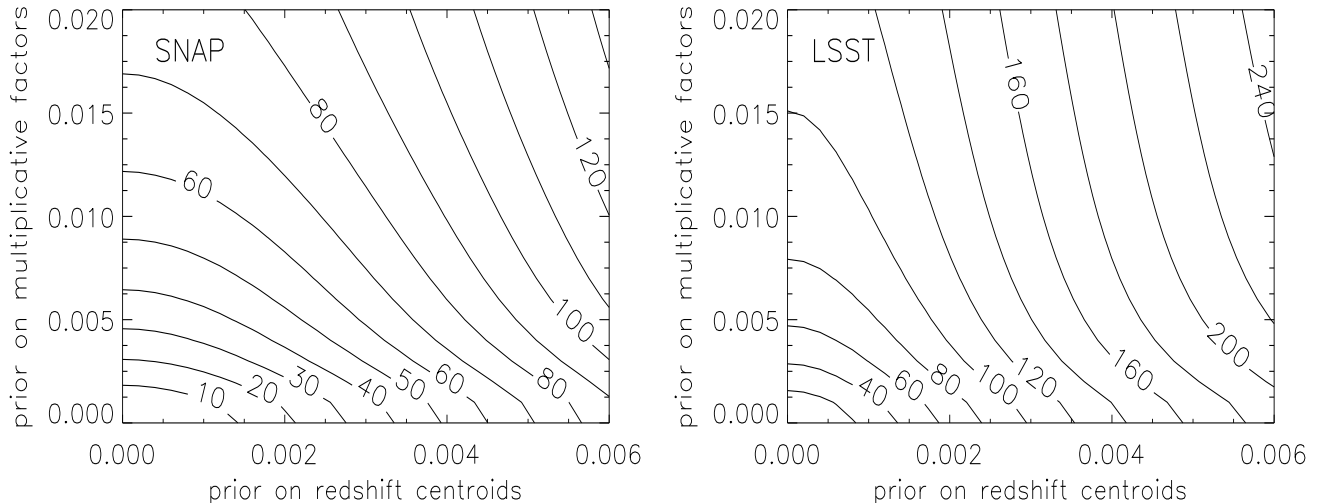


FIG. 8: Contours of constant degradation in equation of state of dark energy w (for the PS case only) with both redshift and multiplicative errors included and for the SNAP fiducial survey (left panel) and LSST (right panel). As before, the degradations are unchanged for a different survey area if we let both errors scale as $f_{\text{sky}}^{-1/2}$. Note that the contours become progressively more vertical at larger values of the redshift error – therefore, the results are weakly affected by the multiplicative errors once the redshift errors become substantial.

important quantity: the individual parameters (say, w_0 and w_a), or their linear combination that is well measured by the survey? We argue that both are needed: the former to understand the behavior of dark energy at any given redshift, and the latter to maximize the constraining power of weak lensing when combining it with other cosmological probes.

For a SNAP-type survey with ~ 100 gal/arcmin², we find that the centroids of redshift bins (of width $\Delta z = 0.3$) need to be known to about $0.003 (f_{\text{sky}}/f_{1000})^{-1/2}$ in order not to lead to parameter degradations larger than $\sim 50\%$. For the LSST-type survey the requirements are about a factor of two more stringent, i.e. $0.0015 (f_{\text{sky}}/f_{15000})^{-1/2}$. These numbers correspond to controlling each Chebyshev mode of smooth variations in $z_p - z_s$ to about $0.001 (f_{\text{sky}}/f_{1000})^{-1/2}$ and $0.0005 (f_{\text{sky}}/f_{15000})^{-1/2}$ respectively. These requirements would easily be satisfied by planned surveys if the bias were due to residual statistical errors, since these surveys will have well over a million galaxies per redshift bin. But it remains a challenge to control the *systematic* biases to this level, presumably by using the spectroscopic training sets.

The multiplicative errors need to be determined to about $0.01 (f_{\text{sky}}/f_{\text{sky,fd}})^{-1/2}$ (or 1% of average shear in a given tomographic redshift bin, for the fiducial sky coverages) for the DES and SNAP. The requirements are about a factor of two more stringent for the LSST. The actual multiplicative error will depend on the galaxy size and shape, and might have spatial dependence as well. The numbers we quote here refer to the post-correction systematic error, averaged over all galaxies and directions in the sky.

The additive errors in shear require more detailed modeling than the multiplicatives, and in particular they require specifying its two-point correlation function (and the three-point function if we are to consider the bispectrum measurements). We constructed a simple model that includes the redshift and angular dependence of the additive power and a coefficient that specifies the effect on the cross-power spectra relative to that on the auto-spectra. In most cases the additive error in each redshift bin needs to be controlled to a few times 10^{-5} , which corresponds to shear variance of $\sim 10^{-4}$ on scales of ~ 10 arcmin ($\ell \sim 1000$). Note too that the additive error cannot be self-calibrated unless we can identify a functional dependence that it must have. Our parameterization of the additive errors is a first step, and improvements can be made once the sources of the additive error are studied in more detail both from the data and via ray-tracing simulations for given telescope designs.

While the systematic requirements are not stringent beyond what one can reasonably hope to achieve with upcoming surveys, perhaps the most encouraging aspect that we highlighted is the possibility of self-calibration of a part of the systematics. In this scheme, weak lensing data is used to concurrently determine both the systematic and the cosmological parameters. The effects of the parameterized systematics can then be marginalized out without the need to know their values (but at the expense of increasing the cosmological parameter errors), leaving only the subtler

systematic effects that were effectively not taken into account with the assumed parameterization. We find that power spectrum measurements can lead to self-calibration with $\sim 100\%$ error degradation in most cases. A promising result is that combining the PS and BS measurements leads to self-calibration with 20–30% degradation, at least for the more poorly-constrained combinations of parameters. Therefore, not only are the fiducial constraints of PS+BS better than those with PS alone, but also the *degradations* relative to their fiducial constraints are smaller in the PS+BS case, simply because the combined PS+BS are more effective in breaking the degeneracies between the systematic and cosmological parameters than the PS or the BS alone. However, we also found that the self-calibration with PS+BS is not nearly as effective if we consider $w = \text{const}$ (or the best-determined combination of w_0 and w_a). More generally, the accurately measured principal component of $w(z)$ does not benefit from self-calibration as much as its poorly measured components. Finally, we only considered the constraints from the PS and BS, without using information from cross-correlation cosmography or cluster counts. Including the latter two methods, which we plan to do in the near future, could further improve the prospects for self-calibration of systematic errors.

Acknowledgments

DH is supported by the NSF Astronomy and Astrophysics Postdoctoral Fellowship under Grant No. 0401066. GMB acknowledges support from grant AST-0236702 from the National Science Foundation, and Department of Energy grant DOE-DE-FG02-95ER40893. We thank Carlos Cunha, Josh Frieman, Mike Jarvis, Lloyd Knox, Marcos Lima, Eric Linder, Erin Sheldon, Zhaoming Ma, Joe Mohr, Hiroaki Oyaizu, Fritz Stabenau, Tony Tyson, Martin White, and especially Wayne Hu for many useful conversations.

APPENDIX A: CHEBYSHEV POLYNOMIALS

We would like to parameterize the bias between the photometric and spectroscopic redshifts, $\delta z \equiv z_p - z_s$, as a function of z_s . This function is expected to be relatively smooth, and one promising way to parameterize it is to use Chebyshev polynomials. Chebyshev polynomials of the first kind $T_i(x)$ ($i = 0, 1, 2, \dots$) are smooth functions, orthonormal in the interval $x = [-1, 1]$, and take values from -1 to 1 . The first two are $T_0(x) = 1$ and $T_1(x) = x$.

One can represent the redshift uncertainty in terms of the first M Chebyshev polynomials as

$$\delta z \equiv z_p - z_s = \sum_{i=1}^M g_i T_i \left(\frac{z_s - z_{\text{max}}/2}{z_{\text{max}}/2} \right) \quad (\text{A1})$$

where z_{max} is the maximum extent of the galaxy distribution in redshift. For convenience, the fiducial values for the extra parameters are taken to be $g_i = 0$ ($i = 0, 1, 2, \dots, M - 1$). Then the derivatives with respect to the nuisance parameters can be computed via $d/dg_k = [d/dz_p][dz_p/dg_k]$.

Figure 9 shows the select three modes (first, second and seventh) of perturbation to the relation between the photometric and spectroscopic redshift.

-
- [1] Aldering, G. et al. 2004, PASP, submitted (astro-ph/0405232)
 - [2] Arfken, G.B. & Weber, H.J. 2000, “Mathematical Methods for Physicists”, Academic Press, 5th edition
 - [3] Bacon, D. J., Refregier, A. R., & Ellis, R. S. 2000, MNRAS, 318, 625
 - [4] Bartelmann, M., & Schneider, P. 2001, Physics Reports, 340, 291
 - [5] Benabed, K., Van Waerbeke, L. 2004, Phys. Rev. D, 70, 123515
 - [6] Bernardeau, F., Van Waerbeke, L., & Mellier, Y. 1997, A&A, 322, 1
 - [7] Bernardeau, F., Colombi, S., Gaztañaga, E., Scoccimarro, R., 2002, Phys. Rep., 367, 1
 - [8] Bernstein, G. 2002, PASP, 114, 98
 - [9] Bernstein, G. 2005, astro-ph/0503276
 - [10] Bernstein, G., Jain, B. 2004, ApJ, 600, 17
 - [11] Bernstein, G. & Jarvis, M. 2002, ApJ, 123, 583
 - [12] Cooray, A. and Hu, W. 2001, Astrophys. J., 554, 56
 - [13] Cooray, A., Hu, W. 2002, Astrophys. J., 574, 19
 - [14] Cunha, C.E., Oyaizu, H., Lima, M.V., Lin, H., Frieman, J., et al. 2005, in preparation
 - [15] Dodelson, S. & Zhang, P. 2005, astro-ph/0501063

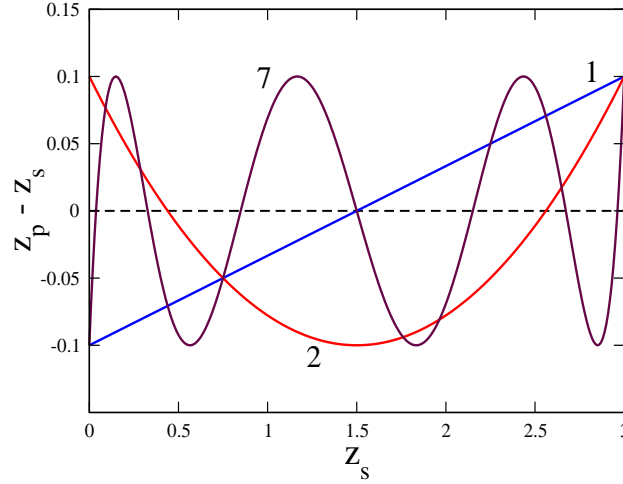


FIG. 9: Select three modes (first, second and seventh) of perturbation to the relation between the photometric and spectroscopic redshift using the Chebyshev polynomials out to $z_{\max} = 3$.

- [16] Dodelson, S., Kolb, E. W., Matarrese, S., Riotto, A., Zhang, P., 2005, astro-ph/0503160
- [17] Eisenstein, D.J. and Hu, W., 1999, ApJ, 511, 5
- [18] Guzik, J. & Bernstein, G. 2005, submitted to Phys. Rev. D
- [19] Hamana, T. et al. 2002, MNRAS, 330, 365
- [20] Heavens, A. 2003, MNRAS, 343, 1327
- [21] Heymans, C., Brown, M., Heavens, A., Meisenheimer, K., Taylor, A & Wolf, C. 2004, MNRAS, 347, 895
- [22] Hirata, C. & Seljak, U. 2003, MNRAS, 343, 459
- [23] Hoekstra, H. 2004, MNRAS, 347, 1337
- [24] Hoekstra, H., Yee, H.K.C. & Gladders, M.D. 2002, ApJ, 577, 595
- [25] Hu, W. 1999, ApJ, 522, L21
- [26] Hu, W. 2003a, Phys. Rev. D, 66, 083515
- [27] Hu, W. 2003b, Phys. Rev. D, 67, 081304
- [28] Hu, W. & Jain, B., 2004, Phys. Rev. D, 70, 043009
- [29] Hu, W. Hedman, M & Zaldarriaga, M. 2003, Phys. Rev. D, 67, 043004
- [30] Hu, W., & Tegmark, M. 1999, ApJ, 514, L65
- [31] Hui, L. 1999, ApJ, 519, L9
- [32] Huterer, D., 2002, Phys. Rev. D, 65, 063001
- [33] Huterer, D., Kim, A., Krauss, L. & Broderick, T. 2004, Astrophys. J., 615, 595
- [34] Huterer, D. & Takada, M. 2005, Astropart. Phys., 23, 369
- [35] Huterer, D. & White, M. 2005, astro-ph/0501451
- [36] Ishak, M. 2005, astro-ph/0501594
- [37] Ishak, M., Hirata, C. M., McDonald, P. & Seljak, U. 2004, Phys. Rev. D, 69, 083514
- [38] Jain, B. & Seljak, U. 1997, ApJ, 484, 560
- [39] Jain, B., Taylor, A.N. 2003, Phys. Rev. Lett., 91, 141302
- [40] Jarvis, M., Bernstein, G., Jain, B., Fischer, P., Smith, D., Tyson, J.A. & Wittman, D. 2003, AJ, 125, 1014
- [41] Jarvis, M., Jain, B., Bernstein, G. & Dolney, D. 2005, astro-ph/0502243
- [42] Jarvis, M., Jain, B. 2004, astro-ph/0412234
- [43] Kaiser, N., Wilson, G., & Luppino, G. A. 2000, astro-ph/0003338
- [44] Kim, A., Linder, E.V., Miquel, R. & Mostek, N. 2003, MNRAS, 347, 909
- [45] Knox, L., Song, Y.-S. & Tyson, A.J. 2005, astro-ph/0503644
- [46] Levine, E.S., Schulz, A.E., & White, M. 2002, ApJ, 577, 569
- [47] Lima, M. & Hu, W. 2004, Phys. Rev. D, submitted (astro-ph/0401559)
- [48] Linder, E.V. & Miquel, R. 2004, Phys. Rev. D, 70, 123516
- [49] Linder, E.V. 2003, Phys. Rev. Lett., 90, 091301
- [50] Ma, Z. & Hu, W. & Huterer, D. 2005, in preparation
- [51] Majumdar, S., & Mohr, J.J. 2003, ApJ, 585, 603
- [52] Mandelbaum, R. et al. 2005, astro-ph/0501201
- [53] Padmanabhan, N. et al. 2005, MNRAS, 359, 237
- [54] Refregier, A., 2003 ARAA, 41, 645

- [55] Refregier, A. et al. 2004, AJ, 127, 3102
- [56] Rhodes, J. et al. 2004, Astropart. Phys., 20, 377
- [57] Rhodes, J. et al. 2004, ApJ, 605, 29
- [58] Schneider, P., Van Waerbeke, L., Mellier, Y. 2002, A&A, 389, 729
- [59] Smith, R.E. et al. 2003, MNRAS, 341, 1311
- [60] Song, Y.-S. & Knox L. 2004, Phys. Rev. D, 70, 063510
- [61] Takada, M. & Jain, B. 2004, MNRAS, 348, 897
- [62] Takada, M. & White, M. 2004, ApJ, 601, L1
- [63] Tegmark, M., Eisenstein, D.J., Hu, W. & de Oliveira-Costa, A. 2000, ApJ, 530, 133
- [64] Vale, C., Hoekstra, H., van Waerbeke, L. & White, M. 2004, ApJ, 613, L1
- [65] Van Waerbeke, L. et al. 2000, A&A 358, 30
- [66] White, M. 2004, Astropart. Phys., 22, 211
- [67] White, M. 2005, Astropart. Phys., 23, 349
- [68] White, M. & Hu, W. 2000, Astrophys. J., 537, 1
- [69] Wittman, D., Tyson, J. A., Kirkman, D., Dell'Antonio, I., & Bernstein, G. 2000, Nature, 405, 143
- [70] Zhan, H. & Knox, L. 2005, Astrophys. J., 616, L75
- [71] Zhang, J., Hui, L., Stebbins, A. 2003, astro-ph/0312348